

PATTERN RECOGNITION OF ROUGH SURFACES BY USING GONIOMETRIC SCATTERED LIGHT

Tobias Geisler, Andreas Kolb

Universität Siegen, Computer Graphics and Multimedia Systems, 57076 Siegen, Germany
(✉ tobias.geisler@uni-siegen.de, +49 212 658 0388, andreas.kolb@uni-siegen.de)

Abstract

Nowadays, most techniques for evaluating rough metal surfaces are based on tactile or confocal measurement procedures. However, these technologies have disadvantages in respect to measuring speeds, resistance to vibration, impact and dust. In this paper we present a novel surface measurement approach, which uses the scattering light technology. Our approach enhances the state-of-the-art scattering light-based surface measurement methodology in both the detector setup and evaluation of the raw intensity values acquired by the scattered light device.

The main goal in optimizing the measurement setup is to capture scattering parameters for rough surfaces in a range greater than $10\ \mu\text{m}$ based on an enlarged detector array. Regarding the evaluation, we propose a pattern recognition approach which maps the reflection intensity I back to material structures and the ten-point mean roughness R_z , the golden standard in tactile roughness characterization. Based on this approach, we are able to classify rough surface deviations like stripes using a simple but robust thresholding.

In order to demonstrate the generality of our approach, we evaluate our approach using two rather different materials, i.e. brushed stainless steel and anodized aluminium.

Keywords: scattered light, rough surfaces, pattern recognition, stripe detection.

© 2018 Polish Academy of Sciences. All rights reserved

1. Introduction

The visual appearance of decorative metal surfaces results from variations in colour saturation and reflection intensities; see Fig. 1. Decorative metal surfaces are used in various applications, e.g. cladding of buildings and furniture or automotive and shipbuilding design. There is a strong request for a technology which enables the online determination of roughness and topographical properties, for example to control the crystalline composition of metal surfaces in series production. Currently, industrial standards for quality assessment for e.g. aluminium profiles, are fully based on subjective appearance considerations of the domain experts [1].

Tactile solutions are the golden standard in this respect, as they are very precise and offer a worldwide quantitative measurement standard, i.e. the R_z -value, as defined in the norm JIS B 0601-2001 [2]. Tactile measurements, however, cannot be applied in series production, as they are restricted in terms of low heat and shock resistance, long acquisition times, and high

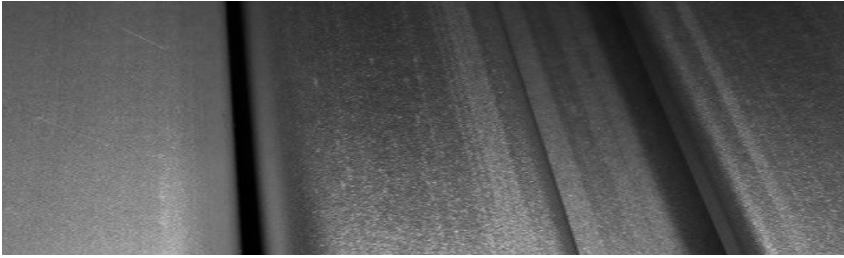


Fig. 1. An illustration of inhomogeneous surface (stripes and colour differences).

costs. The same holds true for contact-free confocal approaches, which can also be used for the estimation of roughness and topographical material properties.

On the other hand, contact-free, camera-based imaging technologies are widely used to directly inspect surface appearance. Examples are image gradient approaches like grey-level gradient co-occurrence matrices (GLGCM), and gradient-only co-occurrence matrices (GOCM), based on the scaled conjugate gradient algorithm, e.g. using machine learning [3]. So far, camera-based approaches have only been applied to the recognition of specific surface patterns, such as stripes and scorings. However, they cannot be used to estimate microstructural and topographical material properties in order to control the production progress towards optimizing the resulting quality of decorative surfaces in colour and structure.

In contrast to the previously described measurement techniques, scattered light approaches have been successfully applied to online monitoring of manufacturing processes of products with glossy and polished metal surfaces. These scattered light techniques are capable of estimating microstructural surface properties, i.e., roughness, topography, colour and appearance [4, 5]. Currently, scattered light techniques are limited when it comes to acquiring rough surface properties even though, in principle, very rough surfaces like brushed stainless steel sheets could be analysed using this technique [6, 7].

In this paper we present an extended approach for measuring surface roughness using the scattered light approach. Our proposed method goes beyond the existing scattered light techniques in the three following aspects. We propose:

- a sensor setup which enables the acquisition of light scattering parameters for rougher surfaces, i.e., we expand the upper limit of detectable roughness from $10\ \mu\text{m}$ to (at least) $15\ \mu\text{m}$,
- a novel approach to recognize surface and reflection patterns on rough surfaces across larger surface areas, such as stripes and scorings, using our light scattering approach, and
- a fast classification approach to the evaluation of material structures according to predetermined R_z quality values.

It should be noted that our improved scattering light technique has the potential to control the manufacturing processes across several production stages, such as electroplating or anodizing materials, and thus it may lead to a significant cost reduction.

The main sections of this paper are presented as follows. In Section 2 we review the previous works on surface measurements by tactile technologies and scattered light. In Section 3 we give an overview of our approach, which implements a quality determination process described in Section 4. First attempts to identify a stripe or a visual figure and their objective derivation are shown in Section 4.4. We conclude the paper with a discussion about the results of our research.

2. State-of-the-art

2.1. Tactile Roughness Measurement

The measurement of surface roughness is traditionally done using conventional measurement stations, based on a slow, tactile surface sampling process. Due to temporal constraints, the tactile approach can hardly be integrated with the online quality control. Usually, a work-piece is (automatically) removed from the production line and moved to the measurement station in order to assess its quality. As tactile measurement is the golden standard in surface quality assessment, methods have been developed in order to directly relate scattered light material parameters to tactile parameters such as the worldwide accepted roughness values: *ten-point mean roughness* R_z and *arithmetical mean roughness* R_a (Fig. 2) [2]. However, this has been done for polished and smooth surfaces only. In this paper, we extend this correlation to significantly rougher materials.

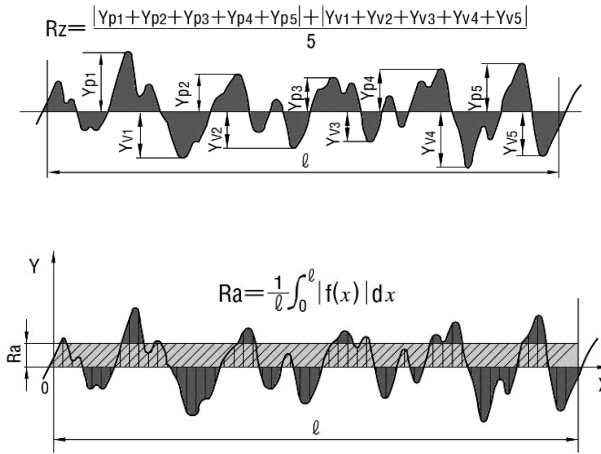


Fig. 2. Arithmetical mean roughness and ten-point mean roughness.

2.2. Light Scattering

Contrary to tactile measurements the *angle-resolved light scattered measurement (ARS)* works contact free and can be used in the online quality control. ARS records reflectance intensities for discrete profile angles φ_i , $i = 1, \dots, n$, backscattered by a small surface region (spot) with diameter d , which in turn is illuminated by an LED. The profile angles φ_i are gathered by a photosensitive linear detector comprising a number n of photodiodes. Fig. 3 depicts this setup which measures the *single reflection intensity* $I(\varphi'_i)$ for an angle φ_i captured at a *normalized position* φ'_i on the detector array, where $\varphi' = \tan(\varphi)$. From this, the *standardized distribution of scattering angles* $H(\varphi)$ and *focus of distribution curve* M are derived [8]:

$$I = \sum_{i=1}^n I(\varphi'_i), \quad H(\varphi_i) = \frac{I(\varphi'_i)}{I}, \quad (1)$$

$$M = \sum_{i=1}^n \varphi'_i * H(\varphi'_i), \quad Aq = \sum_{i=1}^n (\varphi'_i - M)^2 * H(\varphi'_i). \quad (2)$$

The *shape profile* describes the underlying surface topography. It is determined by removing the (high frequency) roughness, by integrating the (high frequency) single reflection intensities yielding a (local) surface orientation. Assuming a perfectly reflecting material, the surface orientation at a surface point is given by $\arctan(M/2)$. Acquiring the number l of measurement spots arranged in a line, the surface profile can be approximated as follows:

$$y = \int_{x \min}^{x \max} \arctan\left(\frac{M(x)}{2}\right) dx \approx \sum_{i=j}^l \arctan\left(\frac{M_j}{2}\right) * \beta x, \quad (3)$$

where β_x is a sampling distance on the surface; see Fig. 3.

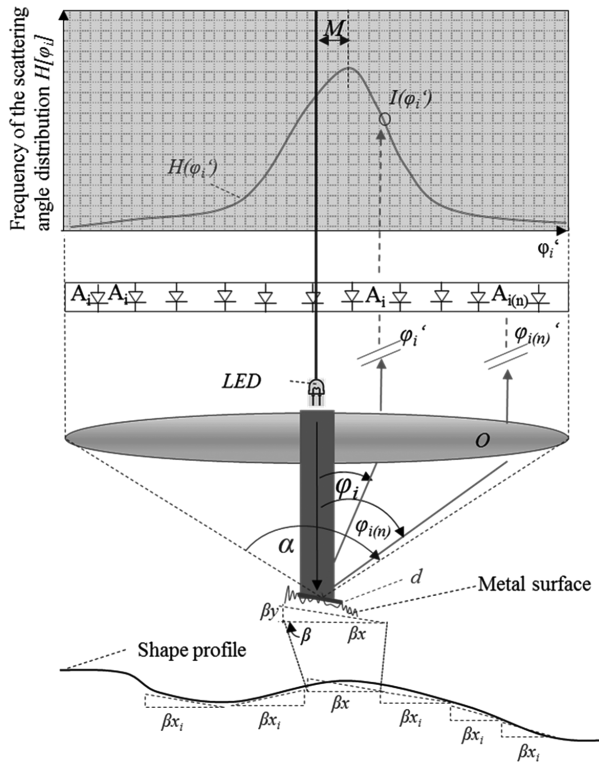


Fig. 3. The ARS measurement principle [8].

Compared with more complex data models for camera- and sensor-based measurement technologies, such as e.g. the Multiple Reflection Cancellation (MRC) algorithm using high order statistics adaptive filters for laser displacement sensors or the Real Peak Detect (RDP) algorithm [9, 10], the analytical scatter models are computationally much less demanding and can often be inverted directly in order to deduce roughness values.

Currently, the limit for acquiring R_z using light scattering devices is $0.1 \mu\text{m}$ for the lowest and $10 \mu\text{m}$ for the highest roughness. In respect to R_a , the upper limit of arithmetical mean roughness is at $1 \mu\text{m}$ [11]. This is due to the fact that for higher roughness values a large portion of light is reflected outside the acquisition angle a of the detector, see Fig. 3. For polished surfaces, standard detectors have an acquisition angle of $a = \pm 16^\circ$ [4].

For a given geometric roughness Rz the optical roughness Aq depends on the material under observation. Commonly, the correlation between Rz and Aq is considered as a surface quality parameter, which, in turn, depends on specific requirements of the production process. This correlation approach enables characterization of surface structures by using light scattering techniques. Unfortunately, analytical models are limited to flat surfaces with low roughness values [11]. Fig. 4, top, shows an almost linear correlation (the dotted trend line) for a grinded shaft steel (HRc 60, diameter 10 mm, finish grinding, $Rz = 1.6 \mu\text{m}$).

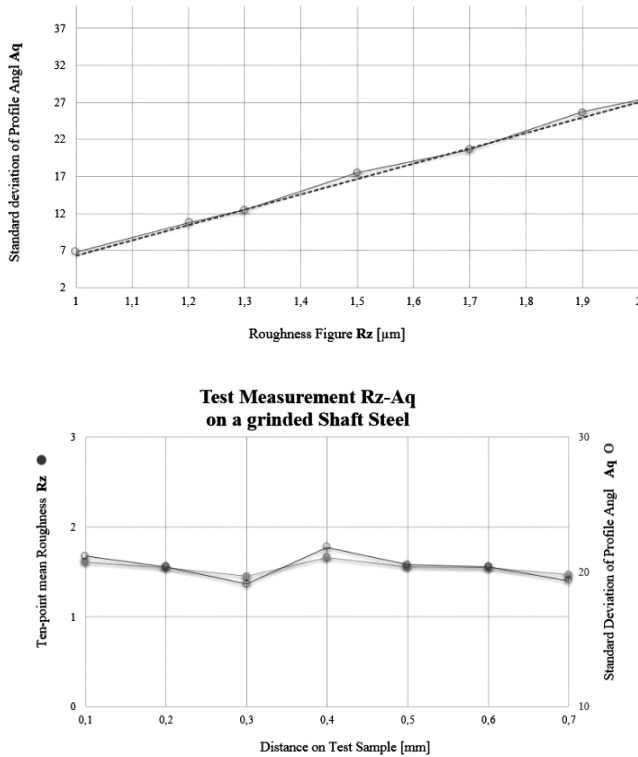


Fig. 4. The measurement accuracy of a Cf53 shaft (hardened and grinded).

Based on the Aq measurement (Fig. 4, bottom) an Rz value of $1.5 \mu\text{m}$ is estimated, which is a slight deviation of the dotted trend line. This is due to the residual error in the linear correlation fitting to Aq . This angle-dependent discrepancy influences the estimation of Rz using Aq ; see Fig. 4, bottom, as this error increases for higher roughness values, due to the loss of reflected light. This is the main reason of why light scattering is mainly used for polished surfaces.

First attempts to apply light scattering methods to higher roughness values and increased roughness ranges have been tested for stainless steel strips in the context of grinding and brushing processes, i.e., the monitoring of abrasion of rollers by measuring the final steel strip roughness [12].

In contrast to the existing methods, our approach is capable to efficiently and accurately acquire larger and rougher surface regions, which makes it applicable to the online quality control. The classification of stripes or inhomogeneous structures requires the evaluation of reflection intensities across larger surface areas, as roughness values alone are not sufficient. Therefore, we

enhance the scattered light technologies to be applicable to rougher surfaces. For the quality classification we deduce quality parameters related to reflection intensities acquired from scattered light, relate them to roughness via double correlation, and apply them to larger areas.

3. Overview of Quality Classification Process

The flowchart in Fig. 5 describes our approach to classify the quality of rough surfaces in respect to a given quality range. The process comprises an offline pre-processing, in which the model material parameters are estimated according to Eqs. (1), (2) using a set of reference workpieces manually classified by the field experts (see Section 4.1). These standard values are material- and application-dependent, as described in Section 4.3.

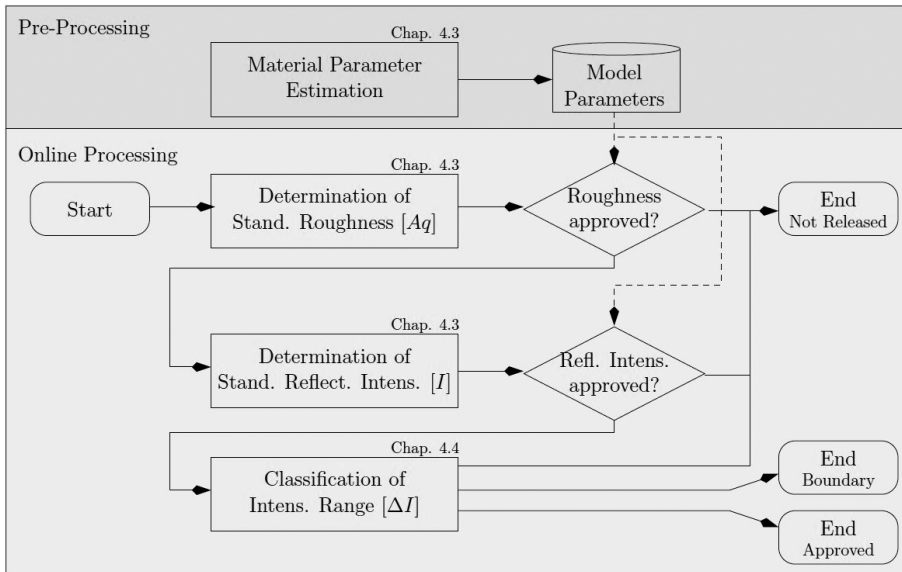


Fig. 5. Our surface classification process based on light scattering.

The online recognition process consists of the following components. In these stages the scattering light parameters of a current workpiece are acquired and compared with the initially determined reference values.

Determination of Standard Roughness: Due to the comparison of the online workpiece parameters with the offline pre-processing parameters a surface can be approved (see Section 4.3). In this case the next classification step “Determination of Standard Reflection Intesity” is applied. If not, the classification is ended and the surface is “Not released”.

Determination of Reflection Intesity: Due to the comparison of the online workpiece parameters with the offline pre-processing parameters a surface can be approved (see Section 4.3). In this case the next classification step “Classification of Intensity Range” is applied. If not, the classification is ended and the surface is not released.

Classification of Intensity Range:

If a surface is approved in the first two stages, the final classification step is applied. This final step includes the area quality assessment (see Section 4.4). Here, we distinguish not only the surfaces

that are in compliance with the reference values (“approved”) and the surfaces exceeding these values (“not released”), but we also distinguish the boundary cases.

The process in Fig. 5 is also described as a pseudo-code algorithm in Section 4.4.

4. ARS Improvement for Robust R_z Estimation

Our main approach in enhancing the scattered light measuring setup is based on a larger photosensitive linear detector with a higher number of diodes. This enables the acquisition of light in a larger field of view (angle α); see Fig. 3. Based on this enhanced measurement we use the standard scattering parameters I and Aq as the basis for our surface classification. We furthermore show an example in which we analyse the homogeneity and structure of rough surfaces, demonstrating the potential of our approach to detect local quality variations, such as stripes.

As an example, we apply our procedure to extruded aluminium alloy AlMgSi0,5 with an anodized surface defined as a 10–15 μm technical oxide layer – natural colour [13], hardness 320 HV and gloss level 20–30 GU-85°. Please note, that the R_z value ranges of our aluminium workpieces clearly exceed the scope of standard scattered light measurement detectors [11].

4.1. Evaluation Setup and Current Limitations

Before we describe our surface classification approach in detail, we give all relevant details on the evaluation procedure in our approach and apply an *OS 500-16* light scattering device from OptoSurf to part of the evaluation. This device comprises a 600 nm LED for illumination focused on a spot of 1.8 mm diameter, an acquisition angle of $\pm 16^\circ$, and a linear detector array with 16 photodiodes.

We have used a *Mitutoyo Surftest 201* stylus instrument as the reference measurement device to acquire R_z values for the offline parameter estimation as well as for evaluation purposes. We have had a set of 90 aluminium workpieces manually approved by the field experts, and a set of 8 negative examples. For all workpieces, 160 point samples along a 20 mm linear section have been acquired for evaluation. We have picked 50 workpieces from the approved set as the *training data* and leave the remaining 40 workpieces as the *test data set*.

In order to demonstrate the current limits, we have measured the 50 training workpiece with the OS 500-16 light scattering device. The result is shown in Fig. 6, top right. For improved visibility, we explicitly display 16 specific $R_z - Aq$ measurements. Apparently, the deviation strongly increases for R_z values above 9 μm , whereas the region below 9 μm exhibits a monotonic increasing behaviour. As the re-mapping from Aq to R_z requires a monotonic fitting function, the non-monotonic $R_z - Aq$ value pairs beyond 9 μm result in the reconstruction error. Thus, estimating R_z is very unreliable beyond 9 μm using the OS 500-16 light scattering device.

4.2. Enhancing Acquirable Scattering Angle

Our goal is to measure rough surfaces. This imposes the necessity to acquire a wider angle of reflected light. This is achieved using an enlarged detector array with 32 photodiodes and an appropriate optics, yielding an acquisition angle of $a = \pm 32^\circ$; see Fig. 3 [14]. Furthermore, acquiring higher surface roughness requires detection of more surface details. The smaller spot size and the larger acquisition angle result in stronger variations of the measurements when moving the device to the next measurement location. Therefore, we have optimized the acquisition algorithm by adding a temporal filter to remove statistical outliers of reflection intensity peaks.

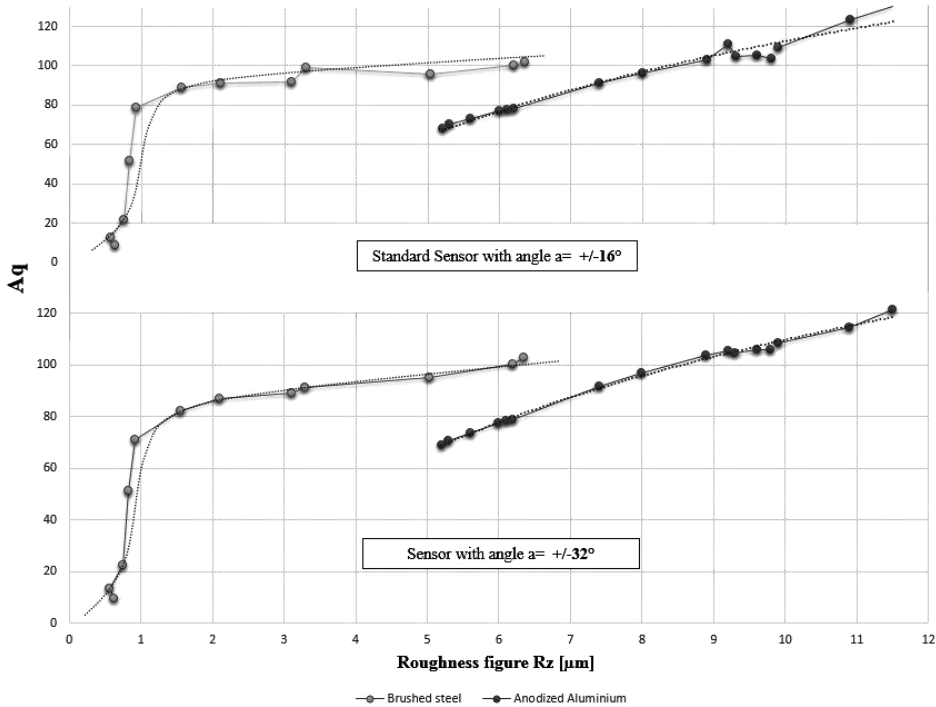


Fig. 6. Comparison of direct correlation $Rz - Aq$ based on $16^\circ/32^\circ$ sensors and data interpolation of rougher surfaces (left: brushed steel / right: anodized aluminium) with a higher inaccuracy range and slope.

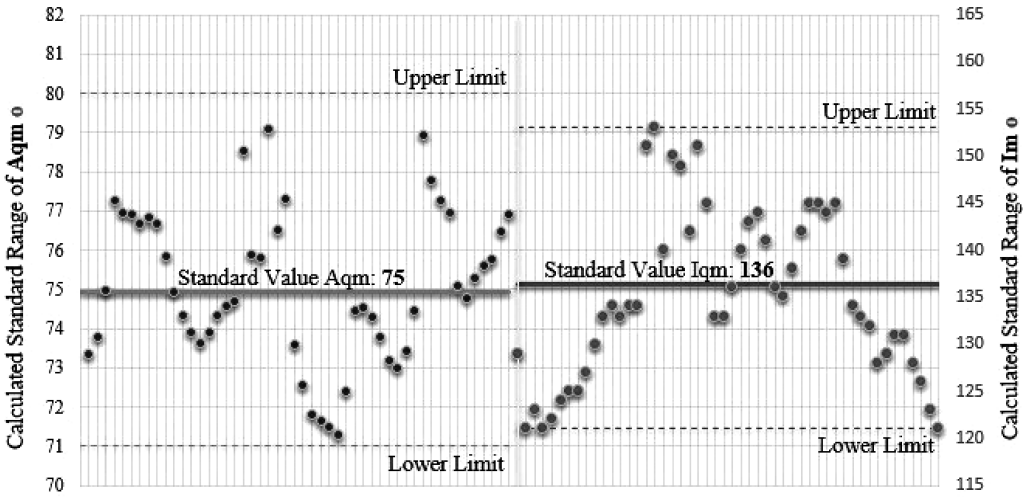
The lower part of Fig. 6 shows the same workpieces of brushed steel as used in Section 2.2 (left) and anodized aluminium surfaces (right) used in Section 4.1 with our modified detector. Due to our technical device improvements, the $Rz - Aq$ relations beyond $9 \mu\text{m}$ are monotonic, leading to a very accurate fit and, subsequently, to a very accurate Rz estimation (see discussion below).

5. Classification of Standard Roughness Aq and Standard Reflection Intensity I

In order to classify the (subjective) appearance of material structures of anodized aluminium surfaces, we have applied the statistical analysis to the (optical) roughness Aq and the reflection intensity I using our 50 training workpieces. The training pieces have been assessed by the domain experts in anodizing, quality assurance and material engineering of an anodizing plant.

First, we have computed the *mean roughness* Aqm as mean of all 160 acquired single Aq values for each of the 50 training workpieces; see Fig. 7, left.

In the same way we have calculated the *mean reflection intensity* Im from the individual intensity values I ; see Fig. 7, right. We have defined the lowest and highest Aqm and Im values within our training set as the limits for approval for a workpiece under examination in the first two stages of our classification process; see Fig. 5. If a current workpiece exceeds these limits, it is not considered for release.



Training Measurement of Approved Samples

Fig. 7. The calculated standard values and limits of rough surfaces.

After Aqm and Im have been determined, the 40 workpieces in our test data set have been used to crosscheck and validate the derived value limits for Aqm and Im ; see Fig. 8. Determination steps can be described as a pseudo-code algorithm, see Section 4.4.

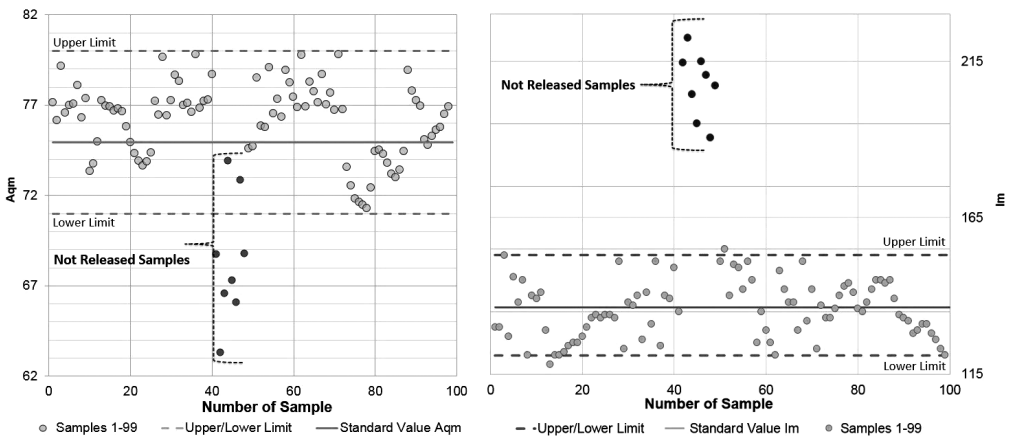


Fig. 8. Cross checks of the calculated standard values and limits.

We have evaluated our measurement results using standard measures from pattern recognition and information retrieval applied to binary classification problems. Classifying the workpieces in the test set, we have obtained the numbers of *true positives* TP and *true negatives* TN , as well as *false positives* (FP) and *false negatives* FN , indicating whether a classification was correct (positive or negative) or incorrect (positive or negative), respectively. Our classification scheme

yields the following results:

$$\text{False Negative Rate} = \text{FN}/\text{cond. Positive} = 0.024 \quad (4)$$

$$\text{Recall} = \text{TP}/(\text{TP} + \text{FN}) = 0.976 \quad (5)$$

$$\text{Precision} = \text{TP}/(\text{TP} + \text{FP}) = 0.930 \quad (6)$$

5.1. Classification of Reflection Intensity Range

So far we have determined the mean roughness A_{qm} and mean reflection intensity I_m in order to classify the quality of a workpiece under examination in a binary manner; see Section 4.3. In the final stage of our process, we have examined the distribution of reflection intensity across the workpiece, aiming at the detection of visible stripe patterns. The identification of quantitative limits particular for stripes is an important first step towards the detection of more complex surface structures in future applications.

The reflection intensity I can apparently be used to detect visual variations along a metal surface. In order to utilize the intensity distribution as a quality measure, we have examined the dependency between the roughness A_q and reflection intensity I . Thus, we have correlated the material composition and visual appearance. Fig. 9 reveals that the A_q values are inversely proportional to those of I .

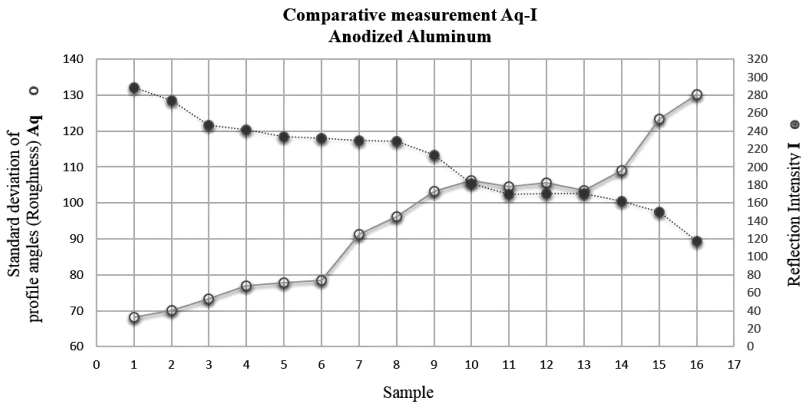


Fig. 9. The results of comparative measurement $A_q - I$ (anodized aluminium).

The observed inverse proportionality between A_q and I results from the optical and material properties of coarse and fine grains on the surface. As grains optically act like micro-mirrors, the areas with dominating coarse grains appear visually smoother, as more light is directly reflected and less light is scattered. On the other hand, the areas with coarse grains have a lower roughness than the areas dominated by fine grains, as roughness mainly appears on grain boundaries.

Due to the observed inverse proportionality and due to the fact that the reflection intensity determines the local spatial reflectivity (see Eq. (1)), we have deduced that it is sufficient to evaluate the surface quality on the basis of the reflection intensity I only.

The perception of colour is very subjective and varies from person to person. It depends on the visual context, i.e., a colour's appearance depends on the surrounding colours and on the lighting environment. In the same way, the perception of stripes on metal surfaces is determined by the contrast of a stripe in respect to its surroundings [15].

In order to determine the final quality of anodized aluminium, we have asked our domain experts to classify the 50 workpieces in our training data set according to the following quality classes: *approved* (a workpiece fully meets the required visual quality assessed by all experts), *boundary* (a workpiece mainly satisfies the required visual quality assessed by most of the experts) and *not released* (a workpiece does not meet the required visual quality).

We have analysed the intensity variation within each of the three classes by determining the *intensity range* $\Delta I = I_{\max} - I_{\min}$ (see Fig. 10). Below you see the complete process as a pseudo-code algorithm:

```

Parameter:
Aqm_{LowerLimit},    Aqm_{UpperLimit},    Im_{LowerLimit},
Im_{UpperLimit}      (see Fig. 7)
For each (i) = each sampling point
Aq(i) = computeRoughness                (see Eq. (2))
I(i) = computeIntensity                  (see Eq. (1))

If Aqm(i) >= Aqm_{LowerLimit} And <= Aqm_{UpperLimit}    [1]
    If Im(i) >= Im_{LowerLimit} And <= Im_{UpperLimit}    [2]
        Select Case I(i)max - I(i)min(see Fig. 10 and Fig. 11) [3]
            Case Is <= 55                                     [4]
                Result ("Approved")                         [5]
            Case 56 To 83                                     [6]
                Result ("Boundary")                         [7]
            Case Else                                         [8]
                Result ("Not Released")                     [9]
        End Select                                          [10]
    Else                                                     [11]
        Result ("Not Released")                             [12]
    End If                                                  [13]
Else                                                       [14]
    Result ("Not Released")                                 [15]
End If                                                    [16]
End                                                        [17]
    
```

Tab. 1 shows the resulting intensity ranges assigned to the three quality classes. Fig. 11 shows a sample intensity profile for the class “not released”. The depicted cross-section shows again the well-established inverse correlation between *Aq* and *I*. Namely, a stripe apparent in the workpiece directly relates to the strong variation of both measures. As expected from visual inspection (see Fig. 11, bottom right), our process classifies the workpiece as “not released”. The sample (bottom right) shows anodized aluminium. A stripe is documented. This surface failure is based on material changing during incorrect punctuality of heat treatment.

Table 1. Definitions of the limit values and quality ranges.

Range Description	Intensity Range $[\Delta I]$
Approved	0–55
Boundary	56–83
Not released	above 83

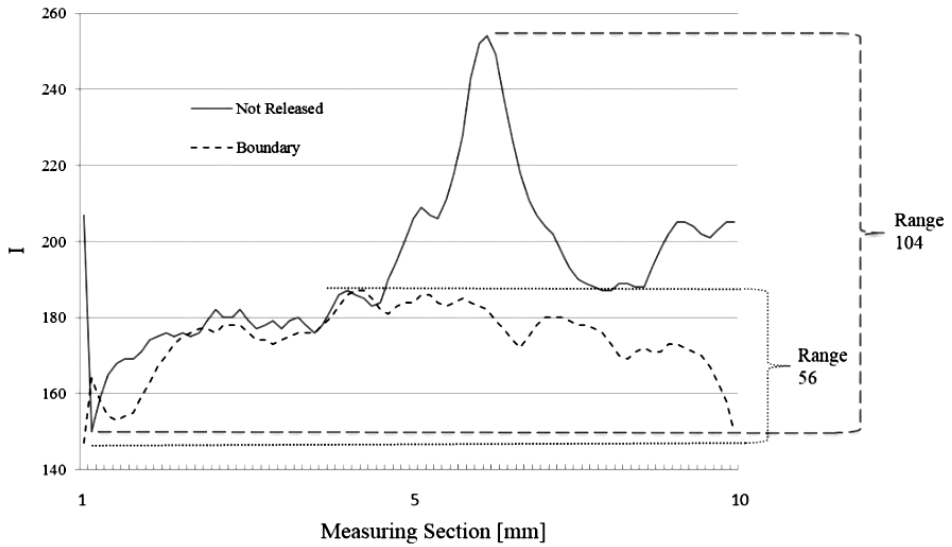


Fig. 10. A sample of quality range measurement.

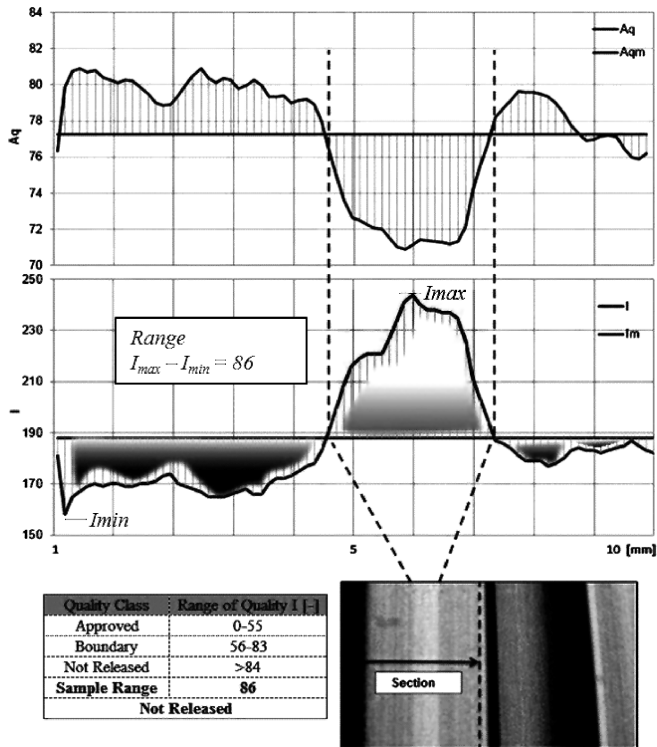


Fig. 11. A sample of stripe detection (anodized aluminium). The spatial variation of A_q and I (top and middle) across the workpiece under inspection (bottom right). The resulting intensity range of 86 workpiece classified as “not released” (bottom left).

6. Conclusions

In this paper we have presented a new method of assessing quality of rough metal surfaces using the scattered light approach. Therefore, we have enhanced the scattered light measuring device in order to acquire a larger field of view in combination with a temporal filtering technique which compensates the increasing amount of statistical outliers. The new setup is limited up to a roughness Rz of $15\ \mu\text{m}$. The current setup works steadily up to Rz of $10\ \mu\text{m}$. Based on the data acquired with this technique, we have applied a two-stage process to classify the surface quality, comprising a thresholding of mean Aq and I values and a variation analysis in order to assess the intensity distribution across the metal surface as the final quality classification. We have successfully applied our method to the stripe detection on anodized aluminium profiles.

Acknowledgements

We would like to thank Andreas Ermertz, quality management at item GmbH, Germany, as well as Jörg Pfordt and Michael Boche, apt Hiller Monheim, Germany, for their support in evaluation of the aluminium samples used in this paper.

References

- [1] DIN Norm. (2014). *Anodized products of wrought aluminium and wrought aluminium alloys*. DIN Norm, DIN 17611:2011–11.
- [2] Volk, R. (2013). *Rauheitsmessung Theorie und Praxis*. Beuth Verlag.
- [3] Chondronasios, A. (2015). *Investigation of surface defects for extruded aluminium profile using pattern recognition techniques*.
- [4] Brodmann, R., Allgauer, R. (1989). Comparison of light scattering from rough surfaces with optical and mechanical profiles. *Proc. Int. Congress on Optical Science and Engineering*, International Society for Optics and Photonics, 111–118.
- [5] Brodmann, R., Thurn, G. (1986). Roughness measurement of ground, turned and shot-peened surfaces by the light scattering method. *Wear*, 109(1–4), 1–13.
- [6] Kaplonek, W., Nadolny, K. (2015). Laser methods based on an analysis of scattered light for automated, in-process inspection of machined surfaces: A review. *Optik – International Journal for Light and Electron Optics*, 126(20), 2764–2770.
- [7] Piln, L., De Chiffre, L. (2015). *Validation of inline surface characterization by light scattering in robot assisted polishing*. Technical report, Technical University of Denmark.
- [8] Norm VDA 2009 2010-07-00. Geometrische Produktspezifikation Oberflächenbeschaffenheit Winkel aufgelöste Streulichtmesstechnik Definition, Kenngrößen und Anwendung.
- [9] Yang, G., Hu, G., Guo, B. (2013). Multiple reflection cancellation using high order statistics adaptive fit for scattered triangulation laser displacement sensor. *Advanced Materials Research*, 774, 1613–1616.
- [10] Kaukoranta, T., Franti, P., Nevalainen, O. (1996). Empirical study on subjective quality evaluation of compressed images. *Electronic Imaging: Science & Technology*, International Society for Optics and Photonics, 88–99.

- [11] Brodmann, R. (2009). *Geometrische Produktspezifikation Oberflächenbeschaffenheit Winkelaufge-
oste Streulichtmesstech-Nik Definition Light Scattering Measurement Tech.* Verband der Automobilin-
dustrie E.V.
- [12] Brodmann, R. (2013). *Robuste Rauheits und Formmessung für die Inline Prozesskontrolle.*
- [13] Jelinek, T. (1997). *Oberflächenbehandlung Aluminium.* Leuze Verlag.
- [14] Brodmann, R. (2014). *Datas Sheet OS 500-32.* OptoSurf GmbH.
- [15] Haralick, R. (2007). Textural features for image classification. *IEEE Transactions on Systems, Man,
and Cybernetics*, SMC-3(6), 610–621.